Electron Injection Study of Photoexcitation Effects on Supported Subnanometer Pt Clusters for CO_2 Photoreduction

Journal:	*Physical Chemistry Chemical Physics*
Manuscript ID	CP-ART-01-2018-000619.R1
Article Type:	Paper
Date Submitted by the Author:	05-May-2018
Complete List of Authors:	Yang, Chi-Ta; University of South Florida, Chemical & Biomedical Engineering Wood, Brandon; Lawrence Livermore National Laboratory, Physical & Life Sciences Bhethanabotla, Venkat; University of South Florida, Joseph, Babu; University of South Florida,

Electron Injection Study of Photoexcitation Effects on Supported Subnanometer Pt Clusters for CO_2 Photoreduction

Chi-Ta Yang,[1] Brandon C. Wood,[2] Venkat R. Bhethanabotla,[3] Babu Joseph[4*]*

[1,3,4]Department of Chemical and Biomedical Engineering, University of South Florida, Tampa, FL, 33620, USA, [2]Materials Science Division, Lawrence Livermore National Laboratory, Livermore, CA 94550, USA.

[1*]chita@mail.usf.edu, [2]brandonwood@llnl.gov, [3]bhethana@usf.edu, [4*]bjoseph@usf.edu,

*To whom correspondence should be addressed: chita@mail.usf.edu; bjoseph@usf.edu.

Keywords: CO_2 photoreduction, Subnanometer clusters, Density Functional Theory, Photocatalyst

Abstract

Using density functional theory, we study the effect of injected electrons (simulating photoexcited electrons) on the energetics, structures, and binding sites available to CO_2 molecules on subnanometer Pt clusters decorated onto anatase TiO_2 (101) surfaces, shedding light on the first and key step of CO_2 photoreduction. Upon the addition of one, two, or three electrons, the O-C-O angles of adsorbed CO_2 become progressively smaller in binding sites that directly contact Pt clusters, while no significant change is found in the intra bond length of the adsorbed CO_2 and in bonding distances between the adsorbed CO_2 and supported clusters. The extra electrons lead to the stabilization of adsorption sites identified on neutral slabs, including previously metastable configurations, suggesting enhancement of accessible CO_2 binding sites. Furthermore, supported clusters are able to populate the electronic states of adsorbed CO_2 species, facilitating the formation of the CO_2^- anion. To help interpret experimentally observed frequencies, conversion factors are proposed to gain insight into the charge state and O-C-O angle of the adsorbed CO_2. Interestingly, upon electron addition, cluster reconstruction may exist due to the bonding inclination between CO_2 and atoms in the Pt cluster, further stabilizing the intermediate complexes. Finally, the rate-limiting step (C-O bond cleavage) in the CO_2 dissociation to CO is slightly reduced by the introduction of an extra electron. Our results show that subnanometer metal clusters based photocatalysts are good candidates for CO_2 photoreduction.

1. Introduction

Harvesting solar energy to convert CO_2 to hydrocarbon fuel addresses two major challenges facing the planet: reducing CO_2 levels in the atmosphere and capturing/storing solar energy.[1-3] According to an Intergovernmental Panel on Climate Change report (IPCC 2007),[4] the atmospheric CO_2 level has been rising at an increasing rate due to the increased consumption of energy. Recently, 81% of energy usage comes from fossil fuels.[3] Renewable fuels production from biomass, wind, solar energy are some possible ways to reduce CO_2 emissions.[2] CO_2 photoreduction via sunlight is a very attractive option, because it addresses these two significant challenges at the same time.[5]

However, one critical issue is the low photo-efficiency,[6] which retards the progress of CO_2 photoreduction toward its practical applications. Of the techniques to improve the photo-efficiency, the deposition of metal particles on a host photocatalyst has drawn significant interest. The nanoparticles can work as co-catalysts to mitigate the recombination of e-/h+ pairs and also as plasmonic particles to increase the concentration of photoexcited electrons.[7, 8] Subnanometer clusters applied to CO_2 photoreduction have recently attracted attention due to their unique properties: dynamic structural fluxionality,[9] larger fraction of under-coordinated surface atoms,[10, 11] and interaction between deposited cluster and the support.[12] These unique properties have shown enhanced catalytic activity in many catalytic reactions.[9, 10, 13-15]

Theoretical exploration can play a significant role in the efficient design of promising photcatalysts.[16] Recently, we have explored the interplay of CO_2, subnanometer Ag and Pt clusters, and TiO_2 surfaces using first-principles calculations toward the design of promising photocatalysts for gas/solid phase CO_2 photoreduction.[17-19] We began with a fundamental study of the interactions of subnanometer Ag and Pt clusters and the TiO_2 support to gain insights into

sintering, encapsulation, and sub-bandgaps[17] that are crucial in (photo)catalysis. The potential of subnanometer Ag clusters on AgBr(110) as a promising photocatalyst was also revealed.[20] The interaction of CO_2 molecules and supported Pt clusters surfaces was then investigated with a focus on the geometry and electronic structure of adsorbed CO_2 species, which sheds light on the first and key step (CO_2 to CO_2^- anion[6, 21]) of the CO_2 photoreduction mechanisms.[18] Prior ab initio studies showed that bent form CO_2 barely adsorbs on TiO_2 surfaces[22-25] except for surfaces with oxygen vacancies exhibiting some adsorption sites.[21, 26] Similar trends were found on other oxide surfaces, such as ceria(110).[27] We further found that Pt octamers deposited on anatase TiO_2 enhance adsorption sites for bent form CO_2, a precursor for the formation of CO_2^- anion.[18] Similar results were obtained on supported Cu clusters.[28] Next, we explored the morphological effect of the 2D and 3D Pt clusters on CO_2 adsorption, thus explaining the structural fluxionality of subnanoclusters;[19] a similar study was also conducted on supported Au clusters.[29] Recently, the CO_2 adsorption dynamics was studied on anatase TiO_2(101) using combined UHV-FTIRS and first-principles calculations,[30] which unveiled more fundamental understandings regarding CO_2 photoreduction, and has suggested corresponding studies on supported subnanometer clusters.

In this article, we study the impact of photoexcited electrons on the interplay of CO_2 and supported Pt clusters. The objectives of this study are to (i) find out whether or not the subnanometer Pt clusters help the transfer of the negative charge to the adsorbed CO_2 to enhance the formation of CO_2^- anions, (ii) investigate energetics and structures of the adsorbed CO_2 species, (iii) see if there is any impact on clusters' morphology upon the electron addition, and (vi) study the effect of extra electron on the CO_2 dissociation to CO. Together with our previous work regarding neutral Pt clusters deposited on TiO_2 surfaces,[18, 19] this study further advances the

design of potential subnanometer metal cluster/semiconductor photocatalysts for CO_2 photoreduction.

2. Computational Methods

Anatase TiO_2 (101) was studied because it is the standard material for the fundamental study of photocatalysis,[31] as well as the main constituent of the widely used commercial photocatalyst (Degussa P25).[32] This surface is characterized by two/three-coordinated O atoms and five/six-coordinated Ti atoms.[17] A 3x1 supercell with six trilayers was considered, in which the bottom three layers were frozen, and the top three layers, Pt clusters, and CO_2 were relaxed. The vacuum region between the slabs was set to 12 Å. The stable CO_2 adsorption sites on perfect and reduced TiO_2 (101) surfaces featuring supported Pt tetramer, hexamer, and octamers were obtained from our previous work.[17, 19] These sites were found on 2D (featuring a planar morphology, approximately 4.30 Å in length and 2.50 Å in width), transition between 2D/3D (featuring a partially planar morphology, approximately 4.70 Å in length, 2.82 Å in width, and 2.50 Å in height), and 3D (approximately 4.69 Å in length, 2.62 Å in width, and 3.00 Å in height).

The DFT calculations were performed using the VASP (Vienna Ab Initio Simulation package) code.[33-35] The Perdew–Burke–Ernzerhof (PBE) functional of the generalized gradient approximation (GGA)[36] was adopted to deal with the exchange-correlation energy. The projector-augmented wave (PAW)[37] method was used for pseudopotentials. A plane wave basis set was used with a cutoff energy of 500 eV. Convergence criteria of the self-consistent loop and force per atom were set to 10^{-5} eV and 0.01 eV/Å, respectively. Spin-polarized calculations were incorporated in all calculations with a Monkhorst-Pack [38] mesh of 2x2x1 k-points.

Past studies simulated the effects of photoexcited electrons either by introducing extra electrons directly into the system with compensating neutralizing positive background charges[21, 24, 39], or by attaching hydrogen atoms that can donate electrons to the conduction band.[21, 40] He et al.[21] studied the energetics of adsorbed CO_2 on anatase TiO_2(101) surfaces upon the addition of one electron, and similar study was investigated on brookite TiO_2 surfaces.[24] The mechanistic steps leading to HCOOH and CO were studied on the bulk TiO_2 surface and a TiO_2 nanocluster upon the addition of electrons;[39] such steps were also studied by attaching a hydrogen atom to the surface 2-fold bridging O atom to simulate photoexcited electrons.[40] Note that He et al.[21] obtained less favorable CO_2 adsorption energies (less negative or more positive, with one exception) using the approach of adding extra electrons to the periodic models as compared to results obtained using the alternative approach of adding hydrogen atoms as the electron source. The calculated amount of charge transfer was comparable using both methods. In our work, photoexcited electrons were simulated by adding electrons to the model systems with compensating positive background charges. The addition of one to three electrons was studied. Note that this approximation assumes complete charge separation of electrons from holes in the photoabsorber. Based on the analysis of He et al.,[21] we expect our results to yield slightly less favored adsorption configurations than would be obtained by the alternative addition of hydrogen atoms.

The Bader charge[41] of the adsorbed CO_2 on supported Pt clusters was analyzed to understand the charge transfer upon electron addition. Density plots and charge density differences with isosurfaces of 0.001 and 0.002e/Å^3, respectively, were studied to gain insights into the cluster reconstruction. The climbing image nudged elastic band method (CI-NEB)[42-44] (Γ point sampling and spin restricted) was used to assess the effect of an extra electron on energy

barrier of CO_2 dissociation to CO. The CO_2 adsorption energies on charged model surfaces were calculated as the difference between the total energy of the composite system (CO_2 adsorbed on charged TiO_2-supported Pt clusters) and the sum of total energies of the isolated CO_2 and charged TiO_2-supported Pt surfaces, more negative adsorption energy indicating more favorable adsorption sites. The vibrational frequencies were calculated using the frozen-phonon approach with a displacement of 0.015 Å for the C and O atoms of the adsorbed CO_2 on the charged model surfaces.

Table 1. Calculated Bader charge of CO_2 adsorbed in site POVo1 (shown in Figure 1) with standard DFT and DFT+U[a]

Ads. Config.	Δe of CO2		
	C	O	O
POVo1	0.595	-0.058	0.039
POVo1_U3p5	0.599	-0.056	0.049
POVo1_U4p0	0.603	-0.067	0.047
POVo1_U4p5	0.599	-0.055	0.053
POVo1(1e)	0.619	-0.066	0.052
POVo1_U3p5(1e)	0.623	-0.065	0.063
POVo1_U4p0(1e)	0.624	-0.064	0.064
POVo1_U4p5(1e)	0.624	-0.066	0.066
POVo1(2e)	0.625	-0.041	0.054
POVo1_U3p5(2e)	0.629	-0.040	0.066
POVo1_U4p0(2e)	0.633	-0.032	0.072
POVo1_U4p5(2e)	0.622	-0.035	0.077
POVo1(3e)	0.657	-0.012	0.064
POVo1_U3p5(3e)	0.659	-0.012	0.075
POVo1_U4p0(3e)	0.659	-0.012	0.076
POVo1_U4p5(3e)	0.659	0.014	0.079

[a]POVo1 represents standard DFT. POVo1_U3p5, POVo1_U4p0, and POVo1_U4p5 represent DFT+U with U values of 3.5, 4.0, and 4.5 eV, respectively (PO representing Pt octamer; Vo representing an oxygen vacancy; 1e-3e representing the addition of 1-3 electrons).

Standard DFT fails to deal with the strongly correlated localized orbitals such as d orbitals of transition metal oxides, resulting in the underestimated bandgap and strongly localized states on the Ti atoms of our models; the DFT+U method[45] is a solution to such issues. To see the difference between DFT and DFT+U on the charge transfer to the CO_2 on the charged TiO_2-supported Pt clusters, a comparison of standard DFT and DFT+U was performed. Previously, a test[18] on neutral anatase TiO_2 (101)-supported Pt octamers with different U values showed little effect (<1% difference in Bader charges). As seen in Table 1, values of U=3.5 eV (which according to the literature[46] best recovers the electronic structure of oxygen vacancy states) up to 4.5 eV show that both DFT and DFT+U lead to comparable results for the Bader charges. Some prior studies have also shown similar trends in the charge distribution and cluster stability using DFT and DFT+U methods for transition metal clusters[47, 48] or binding of adsorbates[49] on perfect or reduced TiO_2 surfaces. Therefore, for simplicity the results in this study were performed without a Hubbard U correction. We underscore that our focus is on understanding trends, which should be well preserved; quantitative measures should therefore be taken with a word of caution due to possible limitations in the chosen method.

Here, we have also neglected explicit thermal effects. Note that thermal effects could alter the geometries of the adsorbed CO_2^- anion and CO_2 species; however, the charge transfer involved in the formation of CO_2^- anion from adsorbed CO_2 species is less likely to be significantly affected, as is the systematic comparison between CO_2 and the CO_2^- anion. In our previous study,[18] we estimated the thermal effect on adsorption by comparing the adsorption energy of CO_2 linearly adsorbed on the TiO_2 surface with an oxygen vacancy (the same simulation method as used in this work) to similar models using NEB and MD simulations.[50] We speculated that values of adsorption energies around or below 0.36eV could become unstable at

room temperature once thermal effects are considered. We also point out that even if thermal effects have little impact on the charge transfer, there is a possibility that a phonon-assisted mechanism could enhance CO_2 dissociation, which would not be captured in the current study.

Another factor that we do not explicitly consider is the role of H_2O molecules, which are known to play a part in CO_2 photoreduction. The interplay of CO_2, H_2O, and the photocatalyst could have an effect on the local geometries of adsorbed CO_2 species. In this case, other interesting CO_2 adsorption configurations may exist, which could help charge transfer to facilitate the formation of the CO_2^- anion. Although beyond the scope of our current investigation, the incorporation of H_2O molecules would be an interesting topic for future study, and the identified adsorption sites and the systematic comparison adopted in our work would help such an investigation aiming at the success of the CO_2 photoreduction.

3. Results and Discussions

To study the effect of photoexcited electrons on the formation of CO_2^- from adsorbed CO_2 species—the first and key step in CO_2 photoreduction—we adopted the method of varying the total charges while introducing uniform compensating background charges. One, two, and three electrons were incorporated into systems of CO_2 adsorbed on stoichiometric and reduced TiO_2-supported Pt tetramers, hexamers, and octamers.[18, 19] In the sections below, we discuss the effect of the extra electrons on four basic ingredients relevant to the success of the first and key photoreduction step:[18] the availability of CO_2 binding sites, corresponding adsorption energy, bent geometry of CO_2, and the charge transfer to adsorbed CO_2. The results are compared with our previous results on neutral model slabs.[18, 19]

A representative set of configurations from our previous work was chosen in order to showcase the effects of the electron injection across a wide variety of Pt cluster sizes and

morphologies on both stoichiometric and reduced TiO_2 supports. Figure 1a-i shows a brief overview of the types of configurations investigated in this study (see Supporting Information (SI), Figure S1-S5 for all configurations investigated except B2 and BVo1 in Ref. 18) and introduces the notation used throughout this text and our previous work[18, 19]. B2 and BVo1 (Figure 1a&b) are reference adsorption sites on TiO_2 without the presence of the metal cluster (bare surface), where the latter includes an oxygen vacancy (Vo). PT2 (Figure 1c) is a site associated with a TiO_2-supported Pt tetramer cluster that is not in direct contact with the cluster. PT1, PTVo1, PHVo1, PH2, PO2, and POVo1 (Figure 1d-i) are Pt-related sites on tetramers, hexamers, and octamers, for which CO_2 contacts either Pt atoms only or else interface edges between Pt atoms and the TiO_2 support.[19] Specifically, PTVo1 and POVo1 are interface edge sites where one O atom in CO_2 is interacting with the surface fivefold-coordinated Ti atom (5c-Ti), while the C or other O atom is in contact with the Pt clusters. PT1, PHVo1, PH2, and PO2 are Pt only sites, among which PT1, PHVo1, and PH2 feature CO_2 interacting with only one Pt atom (1-Pt only), whereas PO2 features CO_2 interacting with two Pt atoms (2-Pt only). In terms of cluster morphology, PTVo1, PHVo1, and PH2 are 2D (featuring a planar morphology), transition between 2D/3D (featuring a partially planar morphology), and 3D morphologies, respectively.[19]

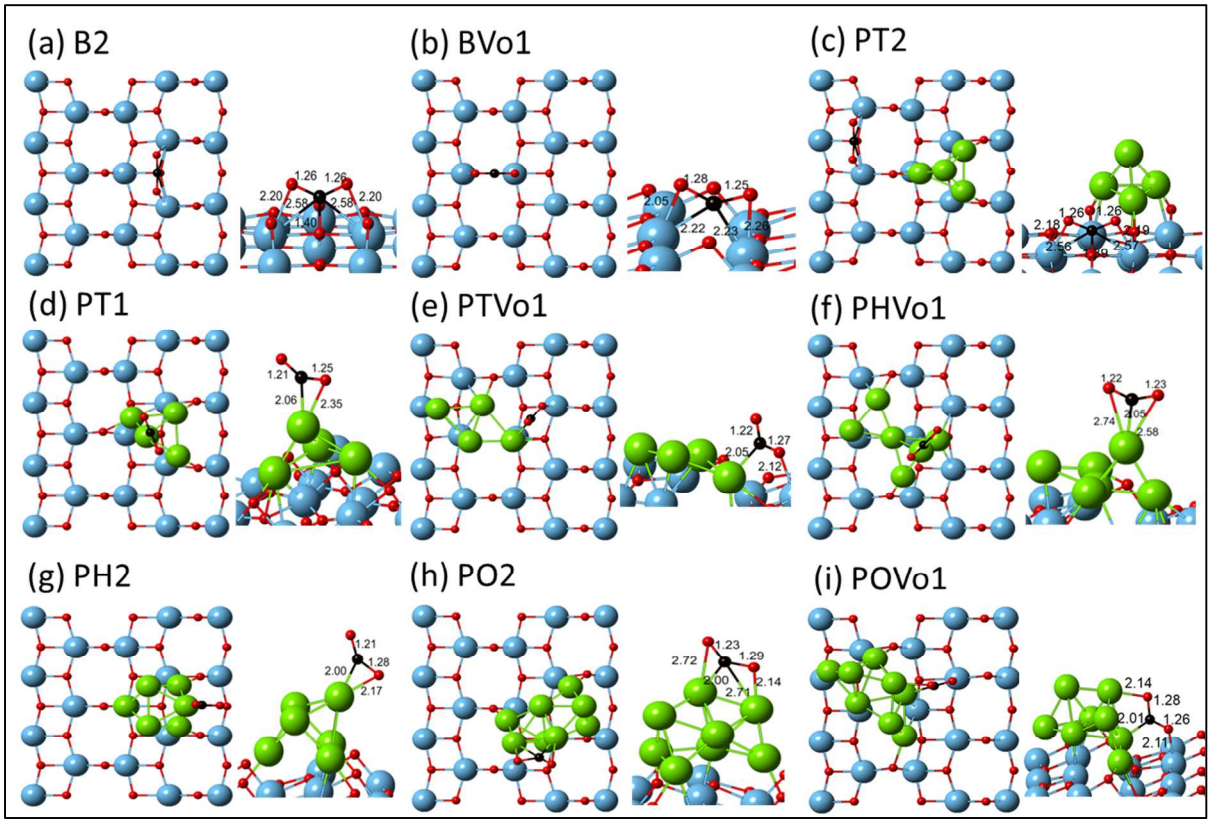

Figure 1. Selected CO_2 adsorption configurations on anatase TiO_2(101) surfaces w/wo Pt clusters upon one electron introduced in the model slabs. The complete configurations investigated in this study are from reference 18 and 19. (B representing TiO_2(101) surface without cluster; PT, PH, and PO represent Pt tetramer, hexamer, and octamer, respectively; Vo represents an oxygen vacancy; O in red, C in black, Ti in blue, and Pt in green. The numbers indicate the bond lengths in Å).

3.1 Effects of Injected e^- on Structural Parameters, Energetics, and Vibrational Frequencies

We begin the discussion with the effect of injected electrons on structural parameters of adsorbed CO_2: the O-C-O angle, intra bond distances of CO_2, and bond distances between CO_2 and the Pt cluster. We then discuss whether the introduced electrons improve metastable and stable CO_2 binding to adsorption sites originally identified on neutral slabs.[18, 19] The formation of CO_2^- anions upon the electron injection is then investigated. The relation between enhanced CO_2 binding and charge transfer is also established. This section ends with the discussion on the

effect on vibrational frequencies, which can be used to reveal geometric and electronic information regarding the adsorbed CO_2 for corresponding experimental studies.

3.1.1 The Effect on Structural Parameters

Observing structures of the CO_2 configurations previously determined to be stable on neutral slabs, the O-C-O angles of adsorbed CO_2 in Pt-related sites have the tendency to become smaller after the addition of electrons. This can be seen in Figures 2a and 2b for interface edge and Pt only sites, respectively. The trend is more dramatic and consistent for Pt only sites; on the other hand, exceptions to the trend (PH3 and POVo4) were observed in interface edge sites.

Unlike the O-C-O bond angle, we find that the change in bond distances of C-O in CO_2, d(C-O), does not have a consistent trend. No more than 5% increase of d(C-O) was observed in some configurations, while other configurations remain almost the same and a few show slight reduction. For the bond distance between O (of CO_2) and Pt, d(O-Pt), no obvious trend was found except for 2-Pt only sites. For the neutral slab, each O of CO_2 on 2-Pt only sites showed an interaction with one Pt atom, but upon the addition of electrons, d(O-Pt) gradually elongates. For the bond distance between C (of CO_2) and Pt, d(C-Pt), a similar effect was observed for 2-Pt only sites: the original tendency of C to interact with two Pt atoms in the neutral system gradually changes with charge addition as C moves to interact with only one Pt atom. These indicate that 2-Pt only sites tend to transform to a configuration of only one O of CO_2 interacting with a Pt atom and C interacting with another different Pt atom. Also, for Pt only sites, d(C-Pt) tends to converge to around 2.00Å after the addition of three electrons. The information of bond lengths can be found in SI Table S1-S5.

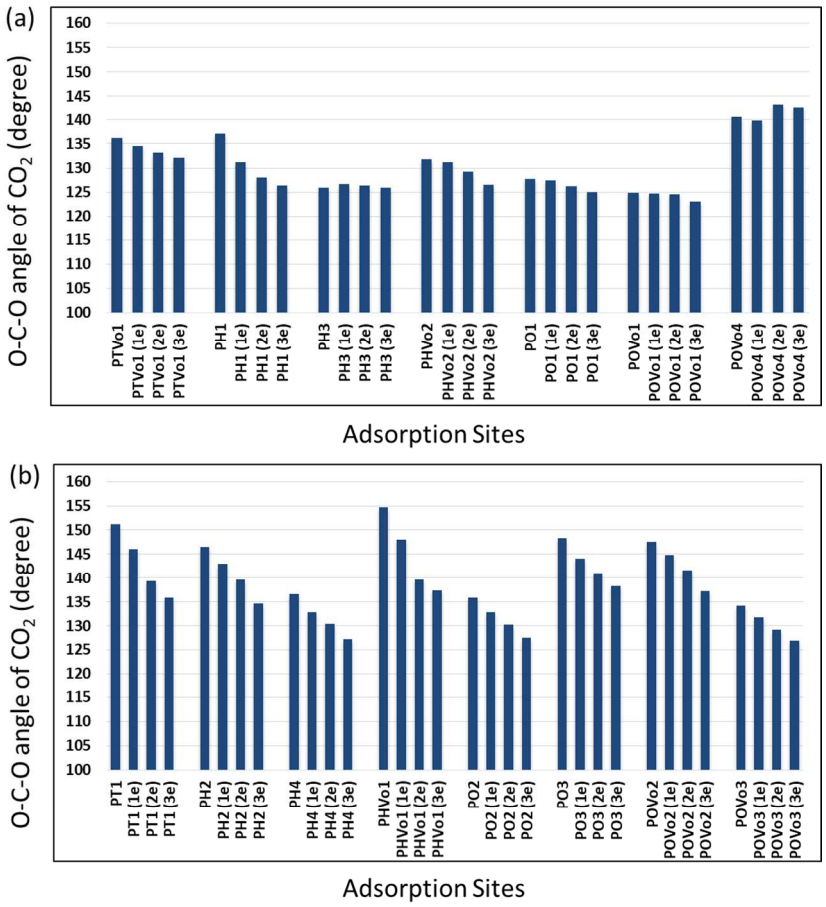

Figure 2. O-C-O angles of stable CO_2 adsorption configurations on neutral and charged anatase TiO_2(101) surfaces in the presence of Pt clusters: (a) interface edge and (b) Pt only sites (PT, PH, and PO represent Pt tetramer, hexamer, and octamer, respectively; Vo represents an oxygen vacancy; 1e-3e represent the addition of 1-3 electrons; the configurations investigated can be found in SI Figure S1-S5).

3.1.2 The Effect on Adsorption Energy

In this section, we discuss the role of excess electrons in altering the adsorption properties of CO_2 on the TiO_2-supported Pt clusters. Upon the addition of electrons, we find that some metastable adsorption sites (originally identified on neutral surfaces[18, 19]) become stable. In addition, for originally stable sites (mainly Pt only & interface edge sites), CO_2 adsorption energy positively correlates with the added electrons for Pt only sites, whereas no such trend was found on interface edge sites. Also, it seems that smaller clusters are more sensitive to the

injected electrons. Notably, these findings suggest that light irradiation would strengthen CO_2 adsorption and improve the availability of binding sites. Accordingly, light irradiation before/during CO_2 introduction to the reaction chamber may be beneficial for improving overall conversion.

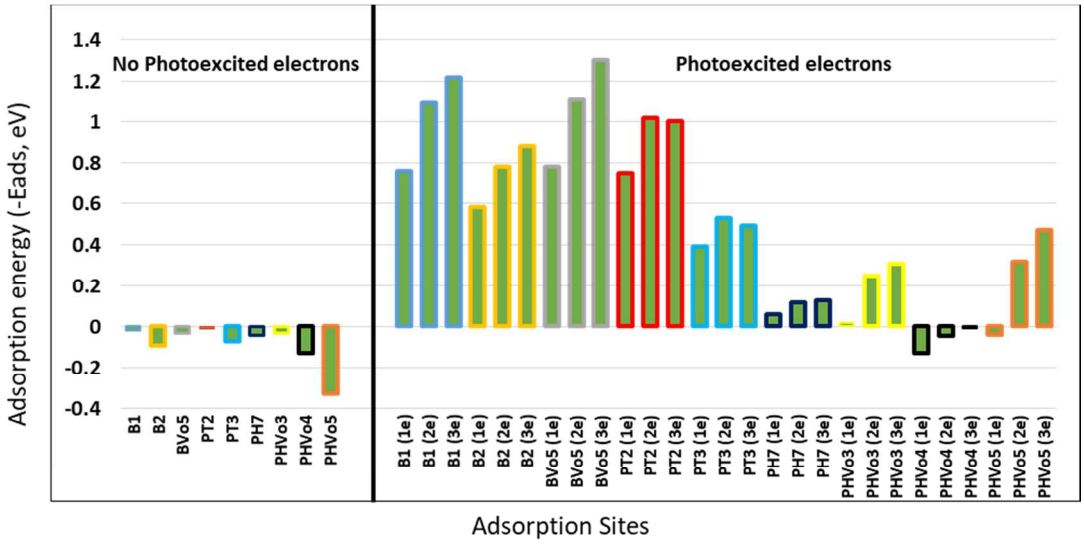

Adsorption Configuration	Explanation of the Notation
B1	CO_2 adsorption on TiO_2, configuration 1 (bent form)
PT2	CO_2 adsorption on TiO_2 – supported Pt tetramer, configuration 2
PHVo3	CO_2 adsorption on TiO_2 (with an oxygen vacancy) – supported Pt hexamer, configuration 3

Figure 3. CO_2 adsorption energies for configurations that were previously found to be metastable on neutral surfaces (left panel) but are stabilized after the addition of electrons (right panel); a table to illustrate the notation (B represents TiO_2(101) surface without Pt cluster; PT, PH, and PO represent Pt tetramer, hexamer, and octamer, respectively; Vo represents an oxygen vacancy; 1e-3e represent the addition of 1-3 electrons; different outline colors indicate different adsorption sites – B1: blue, B2: purple, BVo5: green, PT2: red, PT3: light blue, PH7: dark blue, PHVo3: yellow, PHVo4: black, and PHVo5: dark red; the configurations investigated can be found in SI Figure S1-S5 except B1, B2, BVo5 which can be found in Ref. 18).

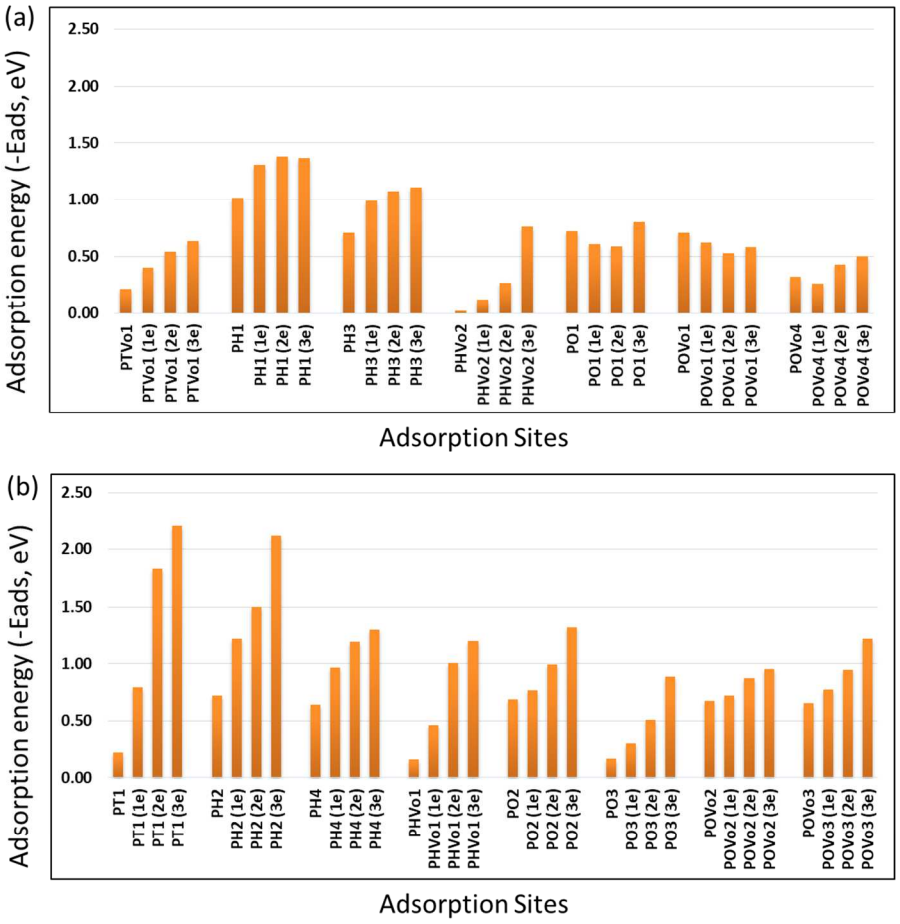

Figure 4. CO_2 adsorption energies for configurations that were previously found to be stable on neutral anatase TiO_2(101) surfaces with Pt clusters. Results are shown before and after electron addition for CO_2 at (a) interface edge and (b) Pt only sites (PT, PH, and PO represent Pt tetramer, hexamer, and octamer, respectively; Vo represents an oxygen vacancy; 1e-3e represent the addition of 1-3 electrons; the configurations investigated can be found in SI Figure S1-S5).

Originally Metastable Sites. Shown in Figure 3 are selected metastable CO_2 adsorption configurations (from neutral slabs) on Pt-free surfaces (B1, B2, and BVo5), as well as on Pt-containing surfaces at sites not directly associated with Pt clusters (PT2 and PT3) and at sites associated with Pt clusters (PH7 and PHVo3-PHVo5). CO_2 adsorption on clean Pt-free surfaces becomes stable upon electron injection, and shows an increasing trend with the amount of added charge. Similar behavior was found for Pt-containing surfaces on sites not directly associated with the Pt clusters. These electrons also help stabilize the CO_2 adsorption associated with Pt

clusters, but the stabilizing effect on these sites is considerably reduced as compared to the other cases. It is revealed that the supported clusters reduce the impact brought by photoexcited electrons.

Originally Stable Sites. The two types of Pt-related sites—interface edge and Pt only sites—behave differently upon electron addition. Shown in Figure 4a are selected interface edge sites. Some of these sites show positive correlation of CO_2 binding with electron injection, while others do not. For instance, PTVo1 and PH3 show increasing CO_2 binding strength, while the effect is mitigated in PO1 and POVo1. All Pt only sites, on the other hand, exhibit positive correlations between CO_2 binding and electron injection, as shown in Figure 4b.

It is clear from the above analysis that the presence or absence of the Pt cluster is a key factor in determining the CO_2 stabilization effect upon the addition of electrons. This stabilization also varies with the cluster size. Both interface edge and Pt only sites on supported Pt tetramer (PTVo1 & PT1) show positive correlations between adsorption energy and electron addition; on supported Pt hexamer (PH1-PH4 and PHVo1 & PHVo2), a similar trend (except PH1) exists. However, in the case of the supported octamers, interface edge and Pt only sites start to behave differently; CO_2 binds strongly as more electrons are added to Pt only sites (PO2, PO3, POVo2 and POVo3), but this trend does not occur in interface edge sites (PO1, POVo1, and POVo4). This reveals that on supported Pt clusters the smaller the cluster is, the more apparent the impact of the introduced electron will be. In general, the extra electrons tend to enhance the CO_2 binding strength, and such enhancement varies in terms of the cluster's presence and the cluster size.

3.1.3 Cluster-Enhanced Charge Transfer

We find that most sites not associated with Pt clusters do not populate electrons to the C of adsorbed CO_2, which is crucial to the formation of the CO_2^- anion.[21] Even though the added electrons may stabilize CO_2 adsorption on sites that were originally metastable on neutral surfaces, the negative charge transfers to those CO_2 molecules are limited. In contrast, supported Pt clusters help electron transfer to the adsorbed CO_2 (especially at Pt only sites) upon electron addition. This is a promising result, because it means supported subnanometer Pt clusters not only provide adsorption sites for bent form CO_2,[18] but also help the electron transfer to bound CO_2 to facilitate the formation of CO_2^- anions. The correlation between charge transfer to CO_2 and its corresponding adsorption energy is also established in this section. Together with previous sections, it is suggested that the irradiation of light can strengthen the CO_2 binding, improve availability of CO_2 binding sites, and facilitate negative charge transfer to C on supported Pt cluster surfaces.

CO_2 Adsorption Directly on TiO_2. Figure S6 in SI illustrates the transfer of negative charges to C of CO_2 regarding sites only in contact with TiO_2. These include B1, B2, and BVo1-BVo5, which are configurations without any clusters, as well as PT2, PTVo2, PO4, and POVo5, which feature CO_2 adsorption directly on the TiO_2 rather than in contact with the clusters. In most cases, injected electrons barely facilitate negative charge transfer to the adsorbed CO_2 (with the exception of BVo4).

CO_2 Adsorption Associated with Pt Clusters. In contrast to sites only in contact with TiO_2, injected electrons are found to facilitate charge transfer to the bound CO_2 when at Pt-related sites, with somewhat different responses for interface edge and Pt only sites. Shown in Figure 5a and 5b are the degrees of negative charge transfer to C of CO_2 in favored interface edge and Pt only sites on supported Pt clusters upon the addition of electrons. Figure 5a reveals

that in general, interface edge sites (PTVo1, PH3, PHVo2, PO1, and POVo1) show an increasing trend of charge accumulation at C in response to electron addition (except PH1 and POVo4). For Pt only sites, shown in Figure 5b, this positive trend is even stronger, indicating that adsorbed CO_2 at these sites has a higher potential to obtain more electrons in response to injected electrons as compared to interface edge sites. In particular, the average accumulation of negative charge gain on C at Pt only sites upon injection of 3 electrons is 38% compared to 11% at interface edge sites. In fact, the lowest percent of negative charge gain among Pt only sites (POVo3, 17%) is comparable to the highest among interface edge sites (PHVo2, 16%). These results reveal the advantage of Pt only sites to facilitate electrons to adsorbed CO_2 once electrons are photo-excited, increasing the success of the first and key step.

The observation that Pt only sites exhibit the strongest dependence on electron injection, both in terms of the relative degree of charge transfer (Figure 5) and CO_2 adsorption energy (Figure 4), can be readily understood by considering that the additional electrons will tend to accumulate on the metal Pt atoms. As a result, CO_2 molecules that have maximal direct contact with these atoms are most likely to be affected. Furthermore, from our previous study, we have shown that the binding of CO_2 in the Pt related sites is facilitated by the hybridization of the bonding molecular orbitals of CO_2 with d orbitals of the Pt atoms.[18] We therefore suggest that the bonding orbitals formed by CO_2 and Pt clusters serve as channels for the negative charge to transfer to the adsorbed CO_2.

Correlation to CO_2 Adsorption Energy. We find positive correlations between the number of injected electrons and the adsorption energy, as well as the negative charge transferred to C of CO_2. We can ask: "Is the enhanced CO_2 adsorption due to the charge transfer to C?" Indeed, comparison of the Pt only and interface edge sites in Figure 4 to those in Figure 5

reveals the existence of a correlation of charge transfer to C with enhanced adsorption energy for some adsorption sites and cluster sizes.

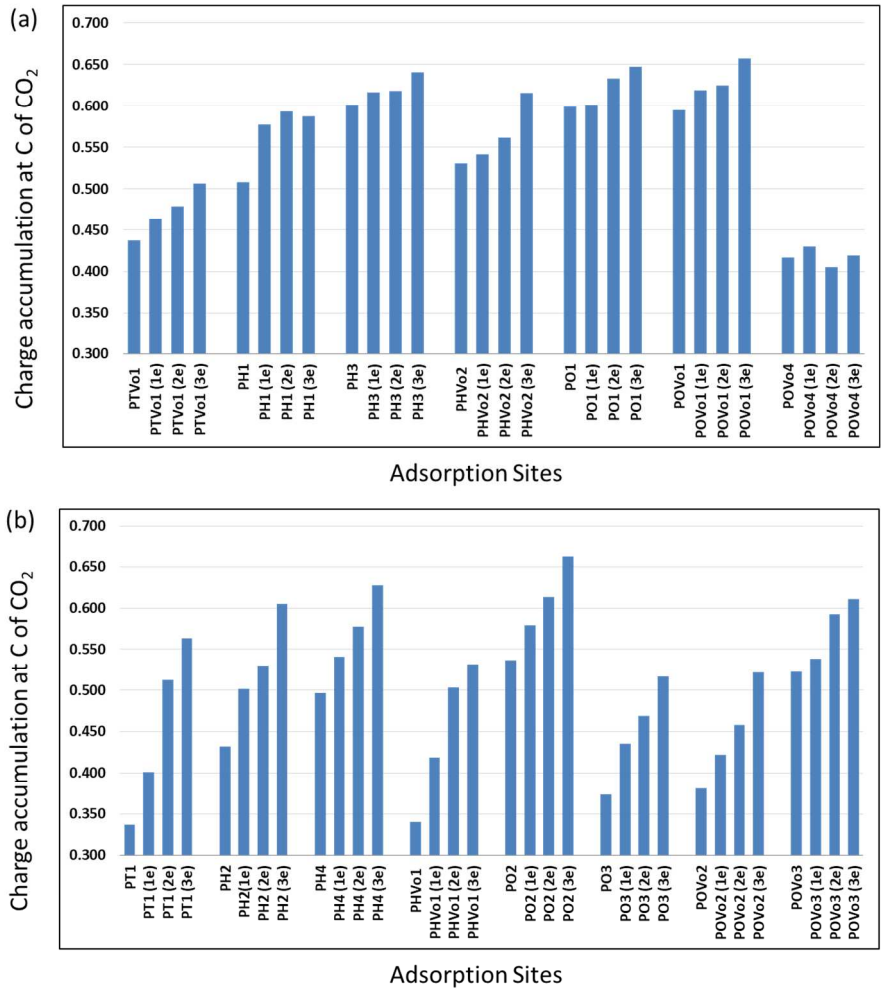

Figure 5. Negative charge accumulation at C of stable CO_2 in sites favored on anatase TiO_2(101)-supported Pt tetramer, hexamer, and octamers upon the addition of electrons at (a) interface edge and (b) Pt only sites (PT, PH, and PO represent Pt tetramer, hexamer, and octamer, respectively; Vo represents an oxygen vacancy; 1e-3e represent the addition of 1-3 electrons; the configurations investigated can be found in SI Figure S1-S5).

Observing all Pt only sites (PT1, PH2, PH4, PHVo1, PO2, PO3, POVo2, and POVo3) in Figure 4b and Figure 5b, we can clearly see that the increase of negative charge to C agrees well with the increase in adsorption energy. This charge increase is believed to maximize the formation of bonding orbitals between C and Pt clusters, leading to enhanced adsorption

energy.[18] However, analyzing interface edge sites (PTVo1, PH1, PH3, PHVo2, PO1, POVo1, and POVo4) shown in Figure 4a and Figure 5a, the correlation starts to become less clear. PTVo1 & PHVo2 show the same correlations and increasing trends exhibited at Pt only sites; PH3 also exhibits a similar correlation and trend. However, the octamers (PO1, POVo1, and POVo4) show no such correlation for interface edge sites. We therefore conclude that there is a strong cluster size dependence for these sites, with smaller clusters tending to exhibit a clearer correlation between charge transfer and absorption energy. We found that the negative charge accumulation per atom of the clusters upon each electron injection is inversely proportional to the cluster size, which may explain why the addition of electrons has stronger impact on smaller clusters. Similarly, larger clusters also provide more closely spaced energy states, and are therefore likely to have a relatively weaker dependence of the energy on the occupation of these states.

The results in Figures 4 and 5 also reveal that cluster size is more of a factor than cluster morphology in determining the degree of correlation between adsorption energy and charge transfer. This is evident because identical trends were observed on all three morphologies considered: 2D (PTVo1), 2D/3D (PHVo2), and 3D (PH1 and PH3) clusters. Furthermore, we caution that the amount of the negative charge at C does not necessarily imply stronger CO_2 adsorption in all cases. Looking at Figure 5a, PHVo2 has a comparable amount of charge accumulation as PH1, and has more charge transfer than that of PTVo1; however, shown in Figure 4a the adsorption energies of these sites do not reflect such charge accumulations. It is likely that each site has its specific charge threshold to sustain CO_2 binding.

3.1.4 Effect on Vibrational Frequencies

Vibrational frequencies[18, 21, 24] computed from DFT models have shown relatively good agreement with experimental results [51, 52] on the spectra of adsorbed CO_2 species. We have proposed using symmetric (ν1), bending (ν2), and asymmetric (ν3) frequencies to gain insights into the negative charge at the adsorbed CO_2, the O-C-O angle of adsorbed CO_2, and identifying adsorption sites.[18, 19] Upon electron addition, we find that vibrational frequencies respond consistently with our previous findings. Shown in Figure 6a and 6b are adsorption sites on stoichiometric and reduced surfaces, respectively, decorated with Pt tetramers, hexamers, and octamers. In general, on all surfaces ν2 increases as more electrons are introduced, and ν3 exhibits the opposite trend. This frequency increase/decrease is attributed to the variations in charge accumulated at C and the O-C-O angles of CO_2.[18, 19] Note that in SI Figure S7, we show that our previously established correlations between ν2 and the negative charge accumulation at C and between ν3 and the O-C-O angle can be extended to incorporate the effect upon the addition of electrons, which suggests the generality of the correlations to incorporate a certain range of the cluster size and charge state of the slabs. From the CO_2 adsorption sites obtained from supported Pt tetramers, hexamers, and octamers on neutral and charged slabs, the vibrational frequencies can be correlated with the electronic and structural information of the adsorbed CO_2 as shown in Table 2. This could be useful in interpretation of experimentally measured values.

Table 2 Suggested conversion factors for converting vibrational frequencies to O-C-O angle and negative charges at C of CO_2

	O-C-O angle of CO_2		Charge at C	
	Slope[a]	Intercept[a]	Slope[a]	Intercept[a]
ν2	-0.1531	243.74	0.0016	-0.6499
ν3	0.0519	46.563	-0.0006	1.4731

[a] Slope and Intercept are based on the equation y= Slope x + Intercept, where y represents O-C-O angle of CO_2 or charge accumulation at C of CO_2, and x represents bending frequency (v2) or asymmetric frequency (v3).

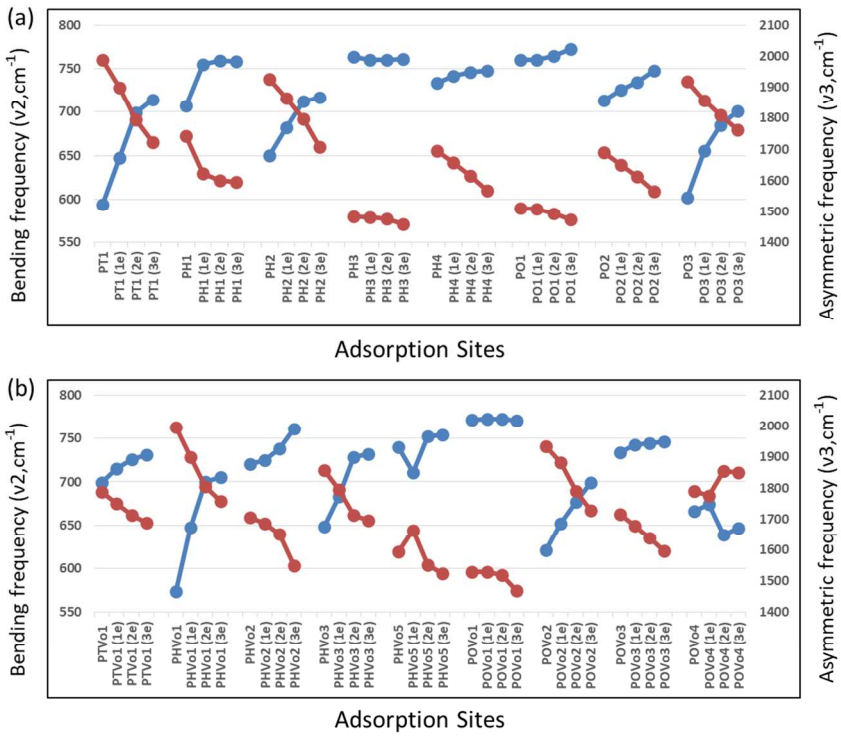

Figure 6. Bending v2 (blue diamond & round dot; left axis) and asymmetric v3 (red cross & dash; right axis) frequencies of CO_2 on supported Pt tetramers, hexamers, and octamers with and without electron addition on (a) stoichiometric and (b) reduced surfaces (PT, PH, and PO represent Pt tetramer, hexamer, and octamer, respectively; Vo represents an oxygen vacancy; 1e-3e represent the addition of 1-3 electrons; the configurations investigated can be found in SI Figure S1-S5).

3.2 Adsorbate Induced Cluster Reconstruction upon Injected Electrons

Imaoka et al.[53] concluded that for nanometer scale (2-10nm) particles, the size is well correlated with the catalytic activity, while for subnanometer scale (0.5-2nm) clusters, the morphology/geometry becomes a dominating factor rather than the size. A recent study regarding Au particles also showed variations in catalytic activities among the individual atom,

monolayer, multilayer and nanoparticle morphologies.[54] The morphology/geometry is thus critical to subnanometeric catalysis.

We find that on the supported Pt hexamer (PH2, 1-Pt only site), the cluster modifies its structure when more and more electrons are injected. We therefore select this configuration for more detailed analysis. As seen in Figure 7a-d, the bond length of Pt1 and Pt4 starts to increase upon the electron addition, and there is an abrupt bond elongation from 2.99 to 3.30Å when two electrons are added. After the addition of three electrons, the bond between Pt1 and Pt4 breaks as CO_2 simultaneously changes its orientation. From the electron density difference of PH2 between the neutral configuration and configurations with additional electrons (Figure 7a-d), it can be seen that the first electron accumulates at Pt6 and CO_2. With three extra electrons, a bonding interaction between CO_2 and Pt6 is established, causing the breaking of the interaction between Pt1 and Pt4. This is believed to drive the reconstruction of the Pt hexamer. The inclination to maximize the bonding interaction between CO_2 and Pt6 directs CO_2 to change its orientation to facilitate stronger adsorption. This enables CO_2 to move Pt4, which CO_2 is tightly bound to, away from its position in the cluster, resulting in cluster reconstruction. Summing the Bader charges of the atoms within the adsorbed CO_2 molecule, we find charge accumulation from -0.30e to -0.41e, -0.53e, and -0.73e going from neutral to one, two, and three electrons, respectively. This implies that more electron addition contributes to stronger bonding between Pt6 and CO_2, which is also reflected in the increasing bonding length between Pt1 and Pt4.

We would like to point out that when more electrons were added to the 2-Pt only site on the supported Pt hexamer (refer to the configuration of SI Figure S3d), no reconstruction was observed. This was even true upon addition of 4 or 5 electrons. One possible reason is that the binding of CO_2 with two Pt atoms restricts CO_2 from changing its orientation, inhibiting possible

formation of bonding interaction between CO_2 with other Pt atoms of the cluster and preventing reconstruction. This suggests that this geometry transformation is site specific, and likely to happen on the sites where the bound adsorbate has sufficient freedom to move (e.g., 1-Pt CO_2 adsorption site).

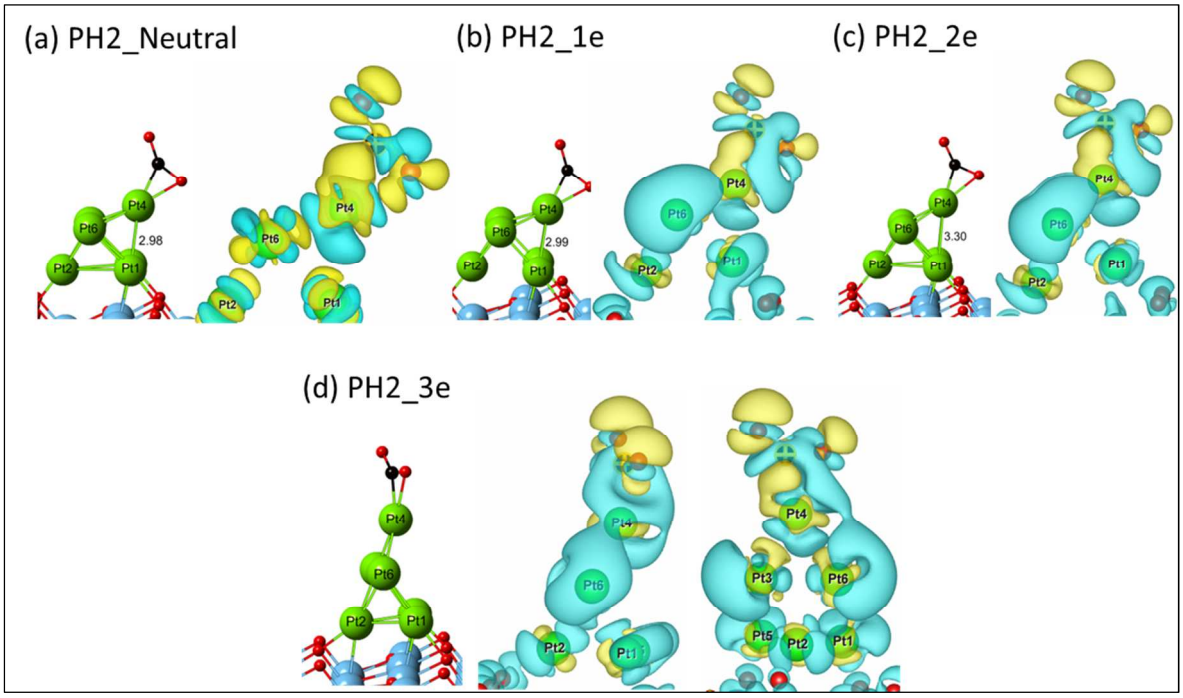

Figure 7. The geometry and electron density difference of CO_2 induced geometry reconstruction of a 1-Pt only site on supported hexamer, PH2 (refer to Figure 1g), upon the addition of electrons from (a) neutral to (c)-(d) one to three extra electrons, respectively. For (d), two different views of the charge density difference are shown for clarity. The electron density difference is based on ρ_{A+B}- ρ_A-ρ_B, where ρ represents electron density, and A and B represents supported hexamer and CO_2, respectively, within the relaxed geometry of the combined A+B system; PH represents Pt hexamer; 1e-3e represents the addition of 1-3 electrons; blue cloud represents negative charge density difference, and yellow cloud represents positive.

3.3 Effect of e^- on CO_2 Dissociation to CO

We previously showed that supported Pt octamers on the neutral anatase TiO_2 surface with an oxygen vacancy can dissociate CO_2 to CO.[18] This can be attributed to the supported Pt cluster's dual effects of filling antibonding orbitals of adsorbed CO_2 to help break the C-O bond, and of

permitting structural fluxionality to help stabilize intermediates and products.[18] Upon the addition of an electron (or photoexcited electron), we find that this behavior is retained, with modest possible enhancement in the predicted kinetics.

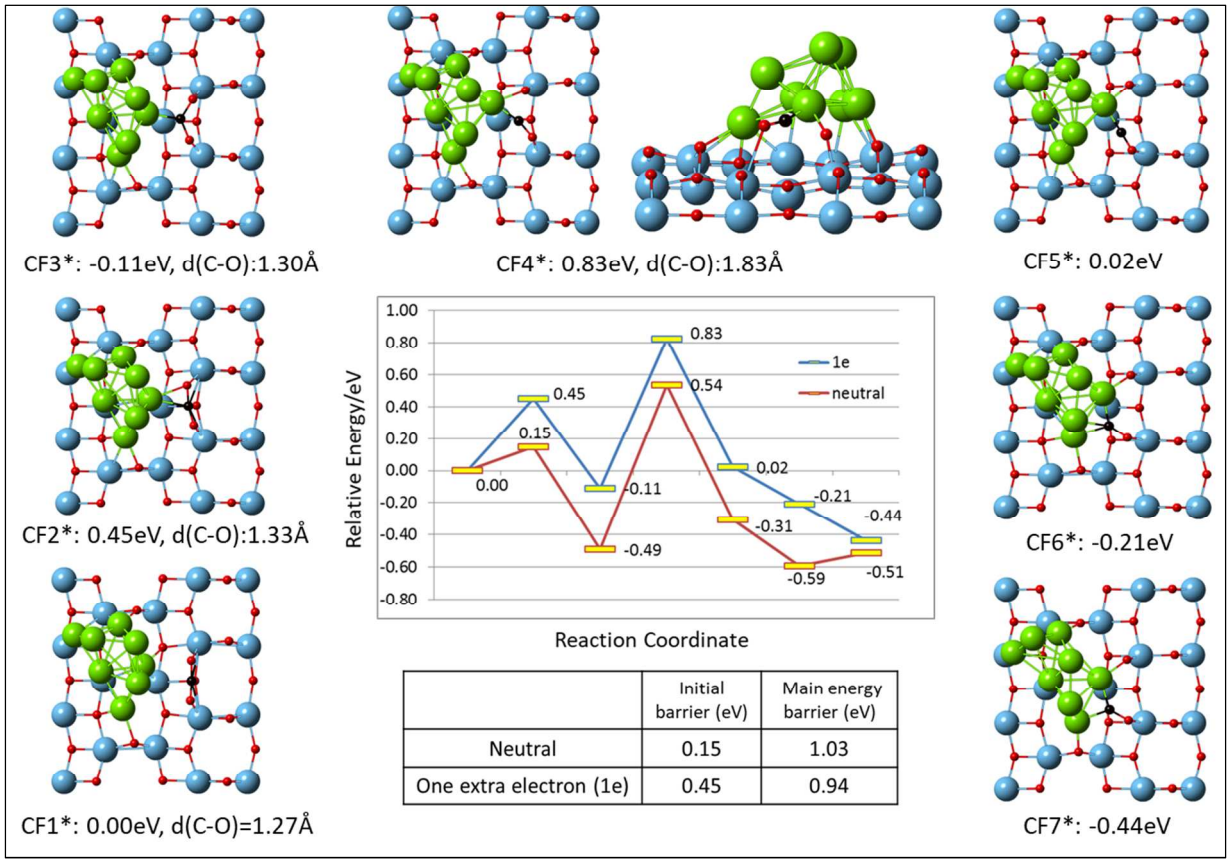

	Initial barrier (eV)	Main energy barrier (eV)
Neutral	0.15	1.03
One extra electron (1e)	0.45	0.94

Figure 8. Structures and energetics of the proposed pathway, CF1*-CF7*, of CO_2 dissociation to CO on reduced anatase TiO_2 (101)-supported Pt octamer with an electron incorporated in the model slab (blue line). The energy landscape for the neutral case[18] is shown for comparison (dashed red line, with consistent calculation parameters).

Figure 8 shows a possible pathway (CF1*-CF7*) for CO_2 dissociation on the supported Pt octamer surface with the incorporation of an extra electron in the model, compared with the neutral case calculated in our previous work.[18] The initial barrier for the transition from CF1* to CF2* is increased by the addition of an electron. This can be explained based on the conclusion in the previous sections that the extra electron enhances the CO_2 adsorption energy, making it

harder to initiate the interactions between Pt octamer and CO_2. The rate limiting step is the C-O bond cleavage step, illustrated in CF3*-CF4*, for which the barrier is slightly reduced with an added electron. This is due to more filling of antibonding orbitals.[18, 55] Taken together, the results in Figure 8 indicate that the effect of the extra electron on CO_2 dissociation is comparatively minor. However, we hypothesize that the C-O bond cleavage step is facilitated by more filling of antibonding orbitals of CO_2. From Figure 5, it is shown that upon adding more electrons, charge will accumulate on CO_2, which should lead to more filling of antibonding orbitals. Therefore, there is reason to believe that when more extra electrons are added to the system, the cleavage of the C-O bond could be enhanced. Moreover, in practice, thermal effects, which are neglected here, may come to play. During the dissociation process, the CO_2 is highly energetic with extra electrons as compared to the neutral case, allowing a phonon-assisted mechanism to possibly enhance CO_2 dissociation. The topics will be left for future study. Note that the energies of the dissociated final states are lower than that of the initial states of the adsorbed CO_2, which thermodynamically favors the spontaneity of the CO_2 dissociation on reduced TiO_2 – supported Pt octamer surface.

4. Conclusions

In summary, we have carried out a systematic study to investigate the potential of subnanometer metal clusters based photocatalysts for CO_2 photoreduction.[17-19] We find that the addition of electrons (simulating photoexcited electrons due to light irradiation) to TiO_2-supported Pt clusters can have a significant effect on the CO_2 adsorption energy, on the availability of binding sites for the bent form of CO_2, and on the charge transfer to form CO_2^- anions.

Among CO_2 adsorption sites associated with the presence of Pt clusters (Pt only and interface edge sites), Pt only sites generally respond more consistently than interface edge sites

upon electron addition. Extra electrons were found to have a significant stabilizing effect on the CO_2 adsorption; sites that were previously identified as metastable for CO_2 adsorption on the neutral surface are stabilized, and the binding of originally stable sites tend to be strengthened. The stronger binding is accompanied by a decrease in the O-C-O angle of adsorbed CO_2. The stabilization of CO_2 binding was further shown to be related to the Pt cluster's presence and cluster size, with relatively stronger CO_2 stabilization observed for smaller clusters.

Our findings suggest that light irradiation on Pt cluster-based photocatalysts strengthens the CO_2 adsorption and enhances the availability of accessible binding sites. Adsorption sites associated with Pt clusters also facilitate the charge transfer to C of the bound CO_2 upon electron addition, which promotes the formation of a CO_2^- anion. This charge transfer correlates with the enhanced adsorption energy, especially in Pt only sites with smaller clusters.

Prior work showed positive correlations between vibration frequency ν2 and charge accumulated at C of CO_2 and between correlation between ν3 and O-C-O angles of CO_2,[18, 19] and we find these trends still hold true upon the addition of electrons. Correlations are proposed to predict angles and charge states of bound CO_2 given the vibrational frequencies. The addition of electrons results in the morphology transformation of certain configurations, including the supported Pt hexamer, which is believed to be due to the extra bonding interaction of CO_2 and Pt clusters. Upon the incorporation of one electron, the slight reduction in the energy barrier of CO_2 dissociation to CO suggests that photoexcited electrons may also somewhat promote this dissociation the surface of supported Pt clusters. Our work offers further support that the deposition of subnanometer metal clusters on photocatalysts is a promising framework of photocatalysts for CO_2 photoreduction. We suggest that computational studies such as these can elucidate mechanistic understandings to help screen and improve potential photocatalysts.

Acknowledgements

The authors wish to thank the USF supercomputing center and MRI support, NSF MRI CHE-1531590, for computing time and support. A portion of this work was performed under the auspices of the U.S. Department of Energy by Lawrence Livermore National Laboratory under Contract DE-AC52-07NA27344. B. C. Wood acknowledges support from Laboratory Directed Research and Development Grant 18-ERD-010. The views and opinions of the authors expressed herein do not necessarily state or reflect those of the United States Government or any agency thereof. Neither the United States Government nor any agency thereof, nor any of their employees, makes any warranty, expressed or implied, or assumes any legal liability or responsibility for the accuracy, completeness, or usefulness of any information, apparatus, product, or process disclosed, or represents that its use would not infringe privately owned rights. The authors would also like to thank VESTA[56] visualization tool for making Figure 7.

ORCID

Babu Joseph: 0000-0003-4094-5917
Chi-Ta Yang: 0000-0001-8265-6422
Brandon C. Wood: 0000-0002-1450-9719
Venkat R. Bhethanabotla: 0000-0002-8279-0100

References

1 P. Usubharatana, D. McMartin, A. Veawab and P. Tontiwachwuthikul, *Ind. Eng. Chem. Res.*, 2006, **45**, 2558-2568.

2 S. C. Roy, O. K. Varghese, M. Paulose and C. A. Grimes, *ACS Nano*, 2010, **4**, 1259-1278.

3 S. N. Habisreutinger, L. Schmidt-Mende and J. K. Stolarczyk, *Angew. Chem. Int. Ed.*, 2013, **52**, 7372-7408.

4 S. Solomon, D. Qin, M. Manning, Z. Chen, M. Marquis, K. Averyt, M. Tignor and H. Miller, *Contribution of Working Group I to the Fourth Assessment Report of the Intergovernmental Panel on Climate Change*, Cambridge University Press, UK and New York, NY, USA, 2007.

5 J. Wei, Q. Ge, R. Yao, Z. Wen, C. Fang, L. Guo, H. Xu and J. Sun, *Nat. Commun.*, 2017, **8**, 15174.

6 V. P. Indrakanti, J. D. Kubicki and H. H. Schobert, *Energy Environ. Sci.*, 2009, **2**, 745-758.

7 S. Linic, P. Christopher and D. B. Ingram, *Nat Mater*, 2011, **10**, 911-921.

8 W. Hou, W. H. Hung, P. Pavaskar, A. Goeppert, M. Aykol and S. B. Cronin, *ACS Catalysis*, 2011, **1**, 929-936.

9 H. Hakkinen, W. Abbet, A. Sanchez, U. Heiz and U. Landman, *Angew. Chem. Int. Ed.*, 2003, **42**, 1297-1300.

10 B. T. Qiao, A. Q. Wang, X. F. Yang, L. F. Allard, Z. Jiang, Y. T. Cui, J. Y. Liu, J. Li and T. Zhang, *Nat. Chem.*, 2011, **3**, 634-641.

11 S. Vajda, M. J. Pellin, J. P. Greeley, C. L. Marshall, L. A. Curtiss, G. A. Ballentine, J. W. Elam, S. Catillon-Mucherie, P. C. Redfern, F. Mehmood and P. Zapol, *Nat. Mater.*, 2009, **8**, 213-216.

12 S. J. TAUSTER, *Acc. Chem. Res.*, 1987, **20**, 389-394.

13 Y. Lei, F. Mehmood, S. Lee, J. Greeley, B. Lee, S. Seifert, R. E. Winans, J. W. Elam, R. J. Meyer, P. C. Redfern, D. Teschner, R. Schlogl, M. J. Pellin, L. A. Curtiss and S. Vajda, *Science*, 2010, **328**, 224-228.

14 B. Yoon, H. Häkkinen, U. Landman, A. S. Wörz, J.-M. Antonietti, S. Abbet, K. Judai and U. Heiz, *Science*, 2005, **307**, 403-407.

15 P.-T. Chen, E. C. Tyo, M. Hayashi, M. J. Pellin, O. Safonova, M. Nachtegaal, J. A. van Bokhoven, S. Vajda and P. Zapol, *J. Phys. Chem. C*, 2017, **121**, 6614-6625.

16 J. K. Norskov, T. Bligaard, J. Rossmeisl and C. H. Christensen, *Nat. Chem.*, 2009, **1**, 37-46.

17 C.-T. Yang, N. Balakrishnan, V. R. Bhethanabotla and B. Joseph, *J. Phys. Chem. C*, 2014, **118**, 4702-4714.

18 C.-T. Yang, B. C. Wood, V. Bhethanabotla and B. Joseph, *J. Phys. Chem. C*, 2014, **118**, 26236-26248.
19 C.-T. Yang, B. C. Wood, V. R. Bhethanabotla and B. Joseph, *Phys. Chem. Chem. Phys.*, 2015, **17**, 25379-25392.
20 Y. Chi, L. Zhao, X. Lu, C. An, W. Guo, Y. Liu and C.-M. L. Wu, *Catal. Sci. Technol.*, 2015, **5**, 4821-4829.
21 H. He, P. Zapol and L. A. Curtiss, *J. Phys. Chem. C*, 2010, **114**, 21474-21481.
22 V. P. Indrakanti, J. D. Kubicki and H. H. Schobert, *Energy Fuels*, 2008, **22**, 2611-2618.
23 A. Markovits, A. Fahmi and C. Minot, *J. Mol. Struct. THEOCHEM*, 1996, **371**, 219-235.
24 M. M. Rodriguez, X. H. Peng, L. J. Liu, Y. Li and J. M. Andino, *J. Phys. Chem. C*, 2012, **116**, 19755-19764.
25 W. Pipornpong, R. Wanbayor and V. Ruangpornvisuti, *Appl. Surf. Sci.*, 2011, **257**, 10322-10328.
26 L. Mino, G. Spoto and A. M. Ferrari, *J. Phys. Chem. C*, 2014, **118**, 25016-25026.
27 Z. Cheng, B. J. Sherman and C. S. Lo, *J. Chem. Phys.*, 2013, **138**, 014702.
28 S. K. Iyemperumal and N. A. Deskins, *Phys. Chem. Chem. Phys.*, 2017, **19**, 28788-28807.
29 L. Liu, Z. Liu, H. Sun and X. Zhao, *Appl. Surf. Sci.,* 2017, **399**, 469-479.
30 Y. Cao, M. Yu, S. Qi, T. Wang, S. Huang, Z. Ren, S. Yan, S. Hu and M. Xu, *Phys. Chem. Chem. Phys.*, 2017, **19**, 31267-31273.
31 M. A. Henderson, *Surf. Sci. Rep.*, 2011, **66**, 185-297.
32 A. Selloni, *Nat. Mater.*, 2008, **7**, 613-615.
33 G. Kresse and J. Furthmuller, *Comp. Mater. Sci.*, 1996, **6**, 15-50.
34 G. Kresse and J. Furthmuller, *Phys. Rev. B*, 1996, **54**, 11169-11186.
35 G. Kresse and J. Hafner, *Phys. Rev. B. Phys.*, 1993, **47**, 558-561.
36 J. P. Perdew, K. Burke and M. Ernzerhof, *Phys. Rev. Lett.*, 1996, **77**, 3865-3868.
37 P. E. Blochl, *Phys. Rev. B*, 1994, **50**, 17953-17979.
38 H. J. Monkhorst and J. D. Pack, *Phys. Rev. B*, 1976, **13**, 5188-5192.
39 D. Lee and Y. Kanai, *J. Am. Chem. Soc.*, 2012, **134**, 20266-20269.
40 H. Y. He, P. Zapol and L. A. Curtiss, *Energy Environ. Sci.*, 2012, **5**, 6196-6205.
41 E. Sanville, S. D. Kenny, R. Smith and G. Henkelman, *J. Comput. Chem.*, 2007, **28**, 899-908.
42 D. Sheppard, R. Terrell and G. Henkelman, *J. Chem. Phys.*, 2008, **128**, 134106.
43 G. Henkelman and H. Jonsson, *J. Chem. Phys.*, 2000, **113**, 9978-9985.
44 G. Henkelman, B. P. Uberuaga and H. Jonsson, *J. Chem. Phys.*, 2000, **113**, 9901-9904.
45 V. I. Anisimov and O. Gunnarsson, *Phys. Rev. B*, 1991, **43**, 7570-7574.
46 W. A. A.-S. Dan C. Sorescu, and Kenneth D. Jordan, *J. Chem. Phys.*, 2011, **135**, 124701.
47 D. Cakir and O. Gulseren, *J. Phys. Chem. C*, 2012, **116**, 5735-5746.
48 Y. Han, M. Zhang, W. Li and J. L. Zhang, *Phys. Chem. Chem. Phys.*, 2012, **14**, 8683-8692.
49 U. Aschauer, Y. B. He, H. Z. Cheng, S. C. Li, U. Diebold and A. Selloni, *J. Phys. Chem. C*, 2010, **114**, 1278-1284.
50 R. Wanbayor, P. Deak, T. Frauenheim and V. Ruangpornvisuti, *J. Chem. Phys.*, 2011, **134**, 104701.
51 W. G. Su, J. Zhang, Z. C. Feng, T. Chen, P. L. Ying and C. Li, *J. Phys. Chem. C*, 2008, **112**, 7710-7716.
52 J. Rasko and F. Solymosi, *J. Chem. Phys.*, 1994, **98**, 7147-7152.
53 T. Imaoka, H. Kitazawa, W. J. Chun, S. Omura, K. Albrecht and K. Yamamoto, *J. Am. Chem. Soc.*, 2013, **135**, 13089-13095.

54 J. Wang, H. Y. Tan, S. Z. Yu and K. B. Zhou, *ACS Catal.*, 2015, **5**, 2873-2881.
55. A. Nilsson, L. G. M. Pettersson, B. Hammer, T. Bligaard, C. H. Christensen and J. K. Norskov, *Catal. Lett.*, 2005, **100**, 111-114.
56 K. Momma and F. Izumi, *J. Appl. Cryst.*, 2011, **44**, 1272-1276.

Graphical and Textual Abstract

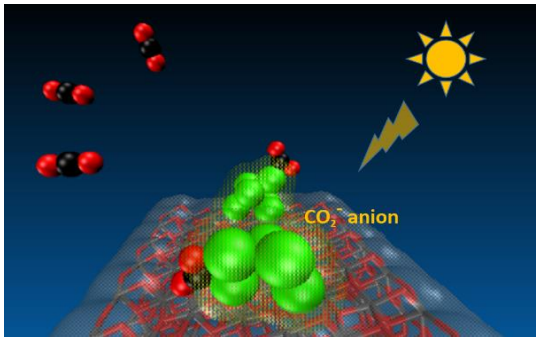

Upon injected electrons, supported Pt clusters stabilize the adsorption of bent-form CO_2 species and facilitate the formation of CO_2^- anions.